Dynamical response function in sodium and aluminum from time-dependent density-functional theory

Marco Cazzaniga,[1,2,*] Hans-Christian Weissker,[2,3,4] Simo Huotari,[5,6] Tuomas Pylkkänen,[5,6] Paolo Salvestrini,[1,7] Giulio Monaco,[5] Giovanni Onida,[1,2] and Lucia Reining[2,3]

[1]*Università degli Studi di Milano, Dipartimento di Fisica, via Celoria 16, I-20133 Milano, Italy*

[2]*European Theoretical Spectroscopy Facility (ETSF)*

[3]*Laboratoire des Solides Irradiés UMR 7642, CNRS-CEA/DSM, Ecole Polytechnique, Palaiseau, France*

[4]*CINaM-CNRS, Campus de Luminy, case 913, F-13288 Marseille Cedex 9, France*[†]

[5]*European Synchrotron Radiation Facility, B.P. 220, F-38043 Grenoble, France*

[6]*Department of Physics, University of Helsinki, P.O. Box 64, FI-00014 Helsinki, Finland*

[7]*CNR-IFN, Physics Department, Politecnico di Milano, piazza Leonardo da Vinci 32, I-20133 Milano, Italy*

(Received 15 November 2010; revised manuscript received 22 March 2011; published 5 August 2011)

We present a detailed study of the dynamical electronic response in bulk sodium and aluminum within time-dependent density-functional theory (TDDFT). The poor results of the random-phase approximation (RPA) and the time-dependent local-density approximation (TDLDA) in sodium are greatly improved by the approximate inclusion of the finite lifetimes of electrons and holes via a modified independent-particle polarizability, which brings the calculated spectra into good agreement with experiment. For aluminum the changes are less visible, but at some values of momentum-transfer lifetime effects are necessary to obtain qualitatively correct spectra. The double-peak structure in aluminum, induced by band-structure effects, is partially washed out by the inclusion of the finite lifetimes. The latter do not, however, create a double peak by themselves as they do in the case of the homogeneous electron gas. Studying the performance of different time-dependent and nonlocal TDDFT kernels, we conclude that the Gross-Kohn, Corradini *et al*., and the Hubbard local-field factors improve the spectra compared to the RPA results. However, the results agree less well with experiment than those obtained using TDLDA with added lifetime effects. These results apply to both the loss spectra and the plasmon dispersion.

DOI: 10.1103/PhysRevB.84.075109 PACS number(s): 78.70.Ck, 71.45.Gm

I. INTRODUCTION

The description of the electronic response in the framework of time-dependent density-functional theory (TDDFT) [1,2] has been successful for different materials and different measurable quantities. In linear-response TDDFT, the exchange and correlation effects in the response are accounted for by the exchange-correlation kernel f_{xc}, for which approximations have to be used.

For finite momentum transfer, the time-dependent local-density approximation (TDLDA) gives a rather good description of the dynamical structure factor measurable in inelastic x-ray scattering (IXS), and of the electron energy-loss function. Here, TDLDA improves distinctly over the random-phase approximation (RPA). This has been demonstrated for a wide range of materials, e.g., Si,[3,4] transition metals,[5] and Al.[6,7] By contrast, TDLDA provides no improvement over the RPA in the long-wavelength limit, i.e., for vanishing momentum transfer,[8] and it cannot reproduce excitonic effects.[9]

Some of us have recently discussed in the case of silicon, the prototypical semiconductor, that TDLDA does not include the effect of the finite lifetimes of the electrons and holes involved in the excitation.[3] However, an approximate inclusion of the lifetimes is possible via a modified independent-particle polarizability χ_0^{LT}. This approach, referred to as TDLDA+LT in the following, leads to excellent results for the IXS spectra.[3,4]

However, this way of describing lifetime effects is not, strictly speaking, compatible with the framework of TDDFT in which the dynamic response is derived from the Kohn-Sham independent-particle polarizability χ_0. All effects beyond the independent-particle response should be introduced by the kernel f_{xc}. It was shown in the case of silicon that the kernel that would describe the same lifetime effects that we introduced via χ_0^{LT} should depend not only on momentum transfer, but also on frequency. Unlike the TDLDA kernel, it should therefore also have an imaginary part.[4]

Several kernels (often referred to as "local-field factors" in many-body perturbation theory) have been derived that have at least one of the characteristics mentioned above. Among them are the Gross-Kohn kernel,[10] the Hubbard local-field factor,[11] and the Corradini *et al*. kernel.[12] These are the kernels we selected to be tested in the present work for their capability to describe realistic spectra.

The main focus of the present work is on the (presumably) simple metal Na. Results are compared throughout the article with the corresponding ones for Al. In the case of aluminum, IXS measurements showing a clear double peak stimulated a number of theoretical and experimental studies covering a wide range of momentum transfers and crystallographic directions.[7,13–15] Our RPA and TDLDA results for Al shown in the present paper essentially reproduce those of Refs. 7 and 14.

The case of sodium is experimentally difficult due to its high reactivity. To the best of our knowledge, only one electron energy-loss measurement was available[16] until recently, as well as a single IXS measurement in Ref. 17. A recent IXS experiment has measured spectra available in a limited range of momenta.[18] A comprehensive experimental study for the case of Na is presented in a separate paper.[19]

On the other hand, previous theoretical studies are limited to the plasmon dispersion, which is very badly described by customary RPA and TDLDA calculations.[6] Quong *et al.* conjectured the polarization of the core electrons to be responsible for these discrepancies.[6] Moreover, to the best of our knowledge, no *ab initio* calculation of spectra for Na is available.

Simple metals have often been discussed as being close to an ideal homogeneous electron gas (HEG). This model neglects the inhomogeneity of the materials on the atomic level and, therefore, all band-structure effects that influence the spectra. However, the calculations based on this approximation do not give satisfactory results even in simple metals. An example of these shortcomings is the double peak in the electron energy-loss spectra of Al and Li. There has been a debate on the origin of this double-peak structure, some authors claiming its origin to be band-structure effects,[20–23] while correlation effects have been put forward by others.[24–34] In particular, Rahman and Vignale[24] have demonstrated that in the HEG the inclusion of quasiparticle lifetimes effects can lead to a double-peak structure.

On the other hand, it has been demonstrated that nontrivial differences are found in the spectra when the band structure of the real materials is used instead of the purely parabolic bands of the HEG.[22,23] In customary *ab initio* TDDFT calculations such as those performed in the present work, the explicit (pseudopotential) description of the electron-ion interaction brings in the inhomogeneity and, therefore, the band-structure effects automatically. The double peak in aluminum clearly derives from band-structure effects, which are sufficiently strong not to be smoothed out completely by the lifetime-induced broadening of the spectra.[19] By contrast, the question on how close the response of sodium is to that of the HEG appears not to have been answered conclusively to date, due to the lack of reliable experimental results for large momentum transfers.

This paper is organized as follows. In Sec. II, we outline the method used in the calculations and the experiment. Subsequently, we present RPA and TDLDA spectra, including details of the lifetime effects, after which the performance of the different available TDDFT kernels is discussed. Finally, we present theoretical results on the plasmon dispersion obtained using the different approximations within TDDFT.

II. METHODS

In the present work, the reference for judging the performance of the different approximations of TDDFT are IXS measurements. This experimental technique measures the double-differential cross section of the scattering of photons into a solid angle range $[\Omega,\Omega+d\Omega]$.[35] The photons transfer a momentum $\hbar\mathbf{Q}$ and an energy $\hbar\omega$ to the sample. The cross section can be written as a product [36]

$$\frac{d^2\sigma}{d\Omega\, d\omega} = \left(\frac{d\sigma}{d\Omega}\right)_{\mathrm{Th}} S(\mathbf{Q},\omega) \tag{1}$$

of the Thomson cross section $(\frac{d\sigma}{d\Omega})_{\mathrm{Th}}$, which is material independent, and the dynamic structure factor $S(\mathbf{Q},\omega)$. All information about the response of the solid is contained in $S(\mathbf{Q},\omega)$. This quantity is connected to the dielectric function ε_{M} by virtue of the fluctuation-dissipation theorem,[37]

$$S(\mathbf{Q},\omega) = -\frac{\hbar Q^2}{4\pi^2 e^2 n}\,\mathrm{Im}\frac{1}{\varepsilon_M(\mathbf{Q},\omega)}, \tag{2}$$

where e and n are, respectively, the electron charge and density, and $Q=|\mathbf{Q}|$.

A. TDDFT calculations

The macroscopic dielectric function is given by the inverse of the diagonal element of the inverse dielectric matrix $\varepsilon^{-1}_{\mathbf{G},\mathbf{G}'}(\mathbf{q},\omega)$ (Refs. 38 and 39)

$$\frac{1}{\varepsilon_M(\mathbf{Q},\omega)} = [\varepsilon^{-1}(\mathbf{q},\omega)]_{\mathbf{G}_q,\mathbf{G}_q}, \tag{3}$$

where $\mathbf{Q}=\mathbf{q}+\mathbf{G}_q$, $\mathbf{q}$ being a wave vector inside the first Brillouin zone and $\mathbf{G}_q$ a reciprocal lattice vector.

The inverse microscopic dielectric matrix is related to the dynamical density-density response function (polarizability) χ by

$$\varepsilon^{-1}_{\mathbf{G},\mathbf{G}'}(\mathbf{q},\omega) = 1 + v_C(\mathbf{q}+\mathbf{G})\chi_{\mathbf{G},\mathbf{G}'}(\mathbf{q},\omega), \tag{4}$$

where v_C is the Coulomb potential. TDDFT in the linear-response regime [1,2] provides a standard method to compute χ. Within this approach, χ is the solution of the Dyson-type equation

$$\begin{aligned}\chi_{\mathbf{G},\mathbf{G}'}(\mathbf{q},\omega) = {}& \chi^0_{\mathbf{G},\mathbf{G}'}(\mathbf{q},\omega) \\ & + \sum_{\mathbf{G}_1,\mathbf{G}_2} \chi^0_{\mathbf{G},\mathbf{G}_1}(\mathbf{q},\omega)[v_c(\mathbf{q}+\mathbf{G}_1)\delta_{\mathbf{G}_1,\mathbf{G}_2} \\ & + f_{\mathrm{xc}\,\mathbf{G}_1,\mathbf{G}_2}(\mathbf{q},\omega)]\chi_{\mathbf{G}_2,\mathbf{G}'}(\mathbf{q},\omega).\end{aligned} \tag{5}$$

The independent-particle response function χ^0 entering in Eq. (5) can be evaluated as

$$\begin{aligned}&\chi^0_{\mathbf{G},\mathbf{G}'}(\mathbf{q},\omega) \\ &= -\frac{1}{V_{\mathrm{BZ}}}\sum_{j,j'}\int_{\mathrm{BZ}} d^3k[f(\epsilon_{j'}(\mathbf{k}+\mathbf{q})) - f(\epsilon_j(\mathbf{k}))] \\ &\quad\times \frac{\langle\mathbf{k},j|e^{-i(\mathbf{q}+\mathbf{G})\cdot\hat{\mathbf{r}}}|\mathbf{k}+\mathbf{q},j'\rangle\langle\mathbf{k}+\mathbf{q},j'|e^{i(\mathbf{q}+\mathbf{G}')\cdot\hat{\mathbf{r}}}|\mathbf{k},j\rangle}{\omega-[\epsilon_{j'}(\mathbf{k}+\mathbf{q})-\epsilon_j(\mathbf{k})]+i\eta},\end{aligned} \tag{6}$$

where $\langle\mathbf{k},j|$ are the Kohn-Sham eigenstates with energy ϵ_j and occupancies f. In the linear-response TDDFT formalism all intricacies of a proper description of many-electron interaction in the response are moved to the exchange-correlation kernel f_{xc}, which is formally defined as the functional derivative of the exchange-correlation potential v_{xc} of DFT with respect to the density ($f_{\mathrm{xc}} = \frac{\partial v_{\mathrm{xc}}(\mathbf{r},t,[n])}{\partial n(\mathbf{r}',t')}$). Similarly to v_{xc}, the exact expression of f_{xc} is unknown and must be approximated. In the present work we consider the following approximations:

(i) RPA, in which χ^0 of Eq. (6) is constructed with the Kohn-Sham band structure and wave functions, and $f_{\mathrm{xc}}=0$. This includes crystal local-field effects via the Coulomb potential but neglects the exchange and correlation contributions.

(ii) Adiabatic local-density approximation (ALDA, also referred to as time-dependent local-density approximation,

TDLDA): χ^0 of Eq. (6) as in (i), but the local, static approximation of the kernel, $f_{\rm xc}(\mathbf{r},\mathbf{r}') = \delta(\mathbf{r}-\mathbf{r}')[dv_{\rm xc}^{\rm LDA}(\rho(\mathbf{r}))/d\rho(\mathbf{r})]$ is used.

(iii) Gross-Kohn kernel, a dynamic extension of TDLDA. The latter corresponds to the static limit of the Gross-Kohn kernel.[10]

(iv) Hubbard kernel: a kernel derived from the many-body local-field factor for the HEG, including exchange effects by a model analytical expression $f_{\rm xc} = -v_c(Q)Q^2/(Q^2+k_F^2)$.[11] For the real solid we use k_F corresponding to the HEG at the average electron density;

(v) Corradini *et al.* kernel: This is a more sophisticate kernel, nonlocal in space, built as a fit on quantum Monte Carlo results.[12]

The following approximation, which has proved successful for IXS spectra of silicon,[3,4] is used to include the effect of the finite lifetimes of the electrons and holes:

(vi) TDLDA+LT, i.e., TDLDA with added lifetime effects. The TDLDA kernel is the same as in (ii). However, we use a modified independent-particle polarizability $\chi_0^{\rm LT}$ in which the imaginary $i\eta$ in the denominator of Eq. (6) is replaced by $i|\mathrm{Im}\,\Sigma_{j'}(\mathbf{k}+\mathbf{q})| + i|\mathrm{Im}\,\Sigma_j(\mathbf{k})|$, Im Σ being the imaginary part of the self-energy. In practice, we retain only the energy dependence of the quasiparticle lifetime by averaging over the Brillouin zone as described in Sec. III B.[3,24]

B. Numerical details

The calculations presented here are performed starting from the DFT ground-state obtained with the ABINIT code[40–42] using the local-density approximation (LDA) for $v_{\rm xc}$. Calculations have been performed using Troullier-Martins pseudopotentials.[40,43] The ground-state calculations were converged adopting a plane-wave cutoff of 16 Ha, a $16\times16\times16$ shifted **k**-point mesh, and a smearing temperature of 0.001 Ha.

The Kohn-Sham eigenvalues and eigenvectors are used as starting point for the TDDFT linear-response calculation, performed by means of the DP code.[44] The integrations over the Brillouin zone for the independent-particle polarizability χ_0 are performed using a $16\times16\times16$ shifted **k**-point mesh. Larger meshes are used to perform the calculations for some **Q** for Al due to the (technical) constraint that **q** has to be the difference of two **k** points in the mesh. We include 40 bands in the calculations which allow a description of the empty states up to ∼45 eV in Na and 85 eV in Al above the Fermi energy. Occupancies are smoothed by introducing an electronic temperature of 5×10^{-4} Ha for Na and 10^{-3} Ha for Al. The momenta smaller than $0.4a_0^{-1}$ require a temperature of 5×10^{-5} Ha for Na and 10^{-4} Ha for Al to converge. The broadening parameter η in the denominator of Eq. (6) is set to 0.2 eV. All spectra are convoluted with a Gaussian of 1 eV full width at half maximum (FWHM) (with the exception of the largest Q for Al, where the FWHM is 2.35 eV) to represent the finite-energy resolution of the experiment.

The response in Na does not depend appreciably on the direction of the momentum transfer. We verified this using test calculations for momentum transfers of equal moduli but pointing in different directions. The direction of the momentum transfer is consequently neglected in sodium. By contrast, all the results for Al are along the [100] direction, since anisotropies have been observed.[13]

C. Measurements

The IXS experiments on polycrystalline Na were performed on the beamline ID16 of the European Synchrotron Radiation Facility.[45] The radiation from the undulators was monochromatized by a Si(111) premonochromator and a Si(220) channel cut. The used photon energies were 9.7–9.8 keV. The spectrometer employed spherically bent Si(660) analyzer crystals. The total energy resolution of the experiment was 1.0 eV, and Q resolution varied between 0.1 and 0.15 Å^{-1}. The tail of the quasielastic zero-loss peak gives uncertainty to the experimental results for $\omega \lesssim 3$ eV. The statistical error bars are smaller than the symbol size in the figures. For further details about the experimental arrangements, see Ref. 19.

III. RESULTS

A. RPA and TDLDA results

We start with the two simplest approximations for $f_{\rm xc}$, RPA and TDLDA, yielding the spectra shown in Figs. 1 and 2. Our RPA and TDLDA results for aluminum are generally in agreement with those of Refs. 7 and 14, while for sodium no spectra are available in literature. At momentum transfers smaller than the plasmon cutoff wave vector Q_c, where the plasmon enters the particle-hole continuum (which is $\sim0.4a_0^{-1}$ in Na and $0.6a_0^{-1}$ in Al) both the numerical and the experimental results show a sharp plasmon peak. Both approximations produce results that are blueshifted with respect to the experiment. TDLDA improves the agreement compared to RPA for both metals. On the other hand, by increasing the momentum transfer Q with the plasmon energy approaching the electron-hole creation region, the agreement worsens: Both the shape and the position of the calculated spectra differ from the measured ones, particularly in RPA. The slight improvement of TDLDA over RPA at these momenta remains unsatisfactory for sodium, while for aluminum the agreement with experiment is better.

For larger momentum transfers, the spectra of Al start to present the well-known double-peak structure.[13,15] In the case of sodium, the experiment does not show this feature.[19] The calculations still present some fine structure, but this is far less pronounced than in the case of Al. This is consistent with the fact that the density of states (DOS) of Na is smooth, and much closer to the HEG DOS than that of aluminum (see Fig. 1 of Ref. 19).

As shown by Sturm *et al.*,[46,47] taking the band structure into account improves the spectra with respect to the HEG results. In order to discuss this point quantitatively, we compare our RPA pseudopotential calculation with the RPA result of the HEG. The main effect of the lattice is a shift of the main structure toward smaller energies. In addition, for the larger momentum transfers considered here, a double-peak structure appears in aluminum, due to a DOS which differs from that of the HEG. By contrast, in the case of sodium, the spectra are rather close to those of the HEG.

Some remarks are in order. There is a small peak-dip structure at ∼8 eV in the aluminum spectra for intermediate

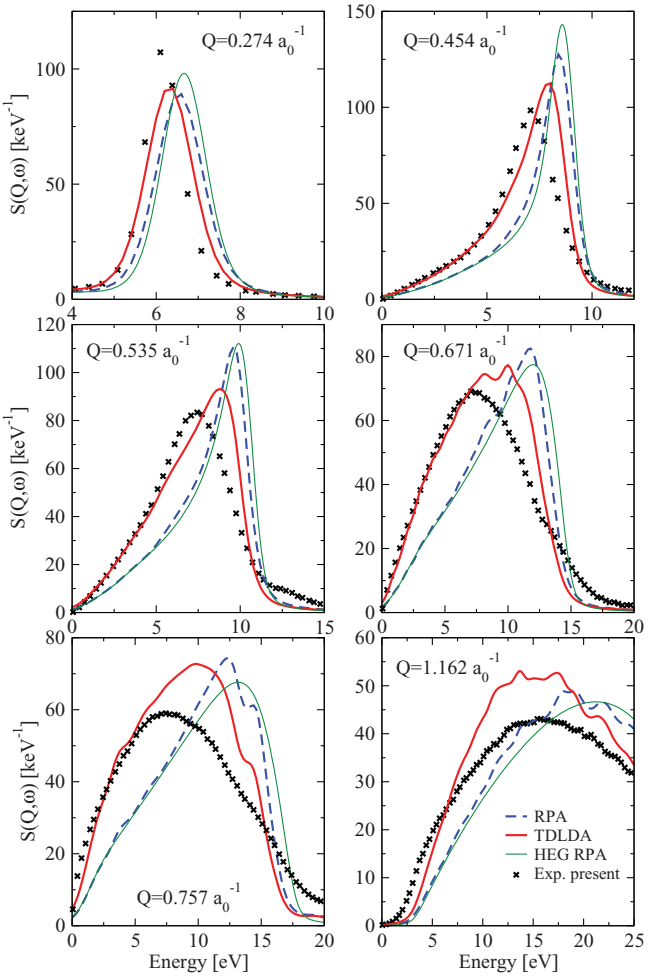

FIG. 1. (Color online) Comparison of the experimental and the calculated dynamical structure factor for sodium. Calculations are performed in RPA and TDLDA. For reference also the HEG RPA (Lindhard) results are plotted. Note that different energy scales are used in the different panels. The plasmon cutoff vector Q_c is $\sim 0.4 a_0^{-1}$.

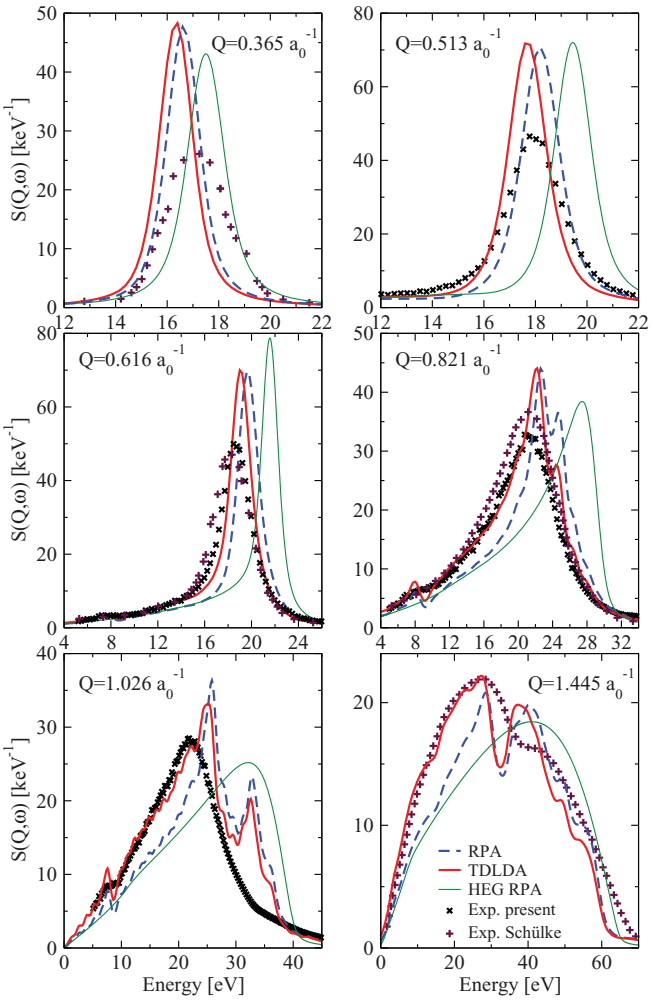

FIG. 2. (Color online) Same as Fig. 1 but for aluminum. Experiments are (a) present work and (b) Schülke *et al.* (Ref. 13). The plasmon cutoff vector Q_c is $\sim 0.6 a_0^{-1}$.

momenta, visible in the spectra for Q between 0.513 and $1.026 a_0^{-1}$. This structure is entirely due to lattice effects, and it is well visible already in the RPA spectra.[15] Conversely, it is completely absent in the HEG result.

On the other hand, in the experimental spectra, a weak structure due to the double-plasmon excitation can be seen in Fig. 1 for intermediate momenta.[18,48] This structure is not present in our theoretical spectra. Our calculations cannot describe the double-plasmon excitation, because the TDLDA kernel is static. Further, many-body effects are needed to describe this structure. Sturm *et al.*[49] considered second- and third-order diagrams in order to do this. In TDDFT one would need a frequency-dependent kernel similar to the case of double excitations in optical spectra.[50]

Moreover, it has been conjectured that the poor agreement between TDLDA spectra and experiment may be due to the influence of core polarization.[6] We have tested this hypothesis using a pseudopotential that includes the $2s$ and $2p$ electrons in the valence. We found that this addition does not result in an appreciable change of the spectra, suggesting that core polarization has little influence on the spectra studied here. More details about core-polarization effects will be published separately.[51]

Finally, although not shown explicitly here, we also found crystal local fields to be negligible throughout the spectra for both metals. This is due to the almost uniform electron density.

B. The inclusion of quasiparticle lifetime effects

The TDLDA kernel does not describe the effect of the finite lifetime of the electrons and holes involved in the excitations. Some of us have shown that the inclusion of lifetime effects via the modified independent-particle polarizability χ_0^{LT}, as described in Sec. II A, greatly improves the results for bulk silicon,[3,4] although for large momentum transfer and energy some discrepancy remains.

Here we apply the same approach to sodium and aluminum. For aluminum, we have calculated the lifetimes within a GW contour-deformation approach.[52] We retain only the energy

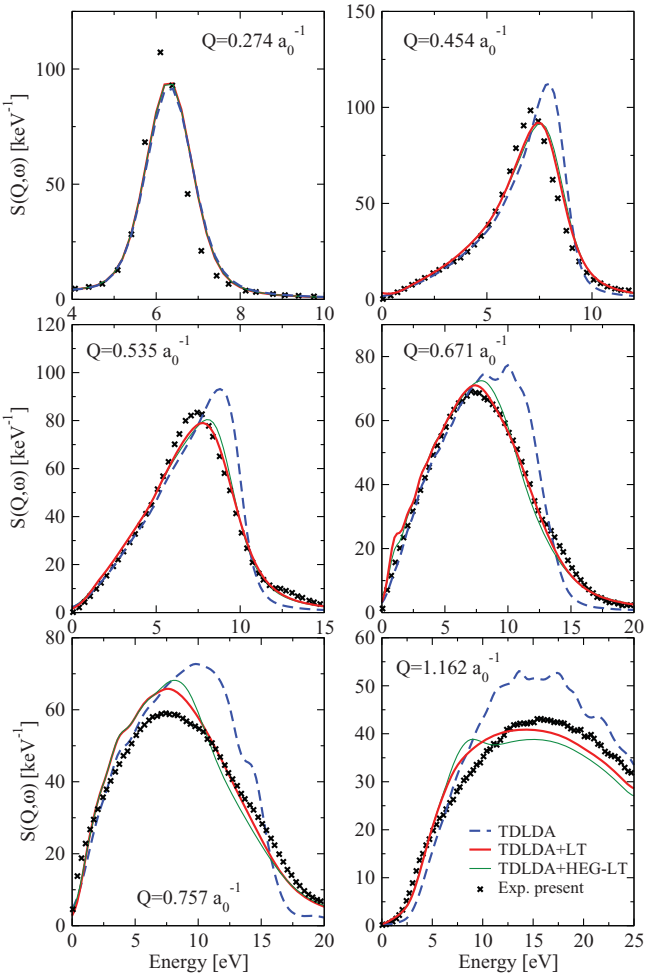

FIG. 3. (Color online) Comparison of experimental and calculated dynamical structure factor for sodium. In TDLDA+LT, the inclusion of lifetimes is done with the lifetimes calculated for Na, while in TDLDA+HEG-LT the lifetimes of the homogeneous electron gas have been used ($Q_c \simeq 0.4a_0^{-1}$). Note that different energy scales are used in the different panels.

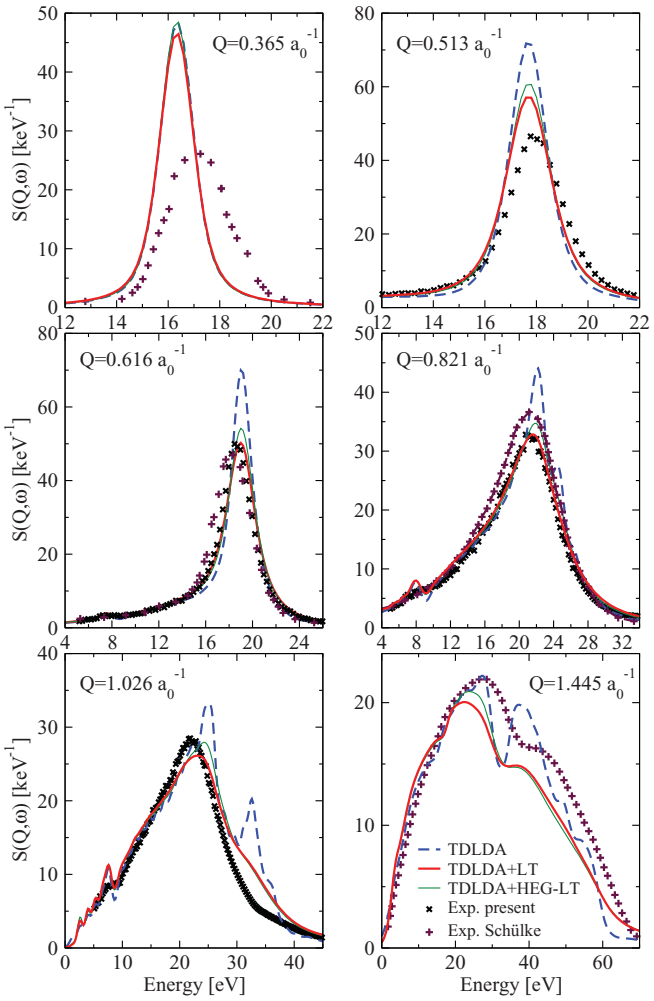

FIG. 4. (Color online) Same as Fig. 3 but for aluminum ($Q_c \simeq 0.6a_0^{-1}$).

dependence, averaging the **k** dependence over the Brillouin zone (BZ) according to

$$\langle \mathrm{Im}\Sigma(\omega)\rangle = \frac{\int_{\mathrm{BZ}} \mathrm{Im}\Sigma(\mathbf{k},\epsilon)\frac{b^2}{(\omega-\epsilon)^2+b^2}d^3k}{\int_{\mathrm{BZ}} \frac{b^2}{(\omega-\epsilon)^2+b^2}d^3k}. \qquad (7)$$

Here b is a parameter to smooth the curve, and ϵ the energy of the DFT-LDA bands. For sodium, we use the imaginary part of the self-energy calculated by Dolado *et al.* and likewise averaged.[53]

The $S(\mathbf{Q},\omega)$ calculated in TDLDA with and without the inclusion of the lifetimes is shown in Figs. 3 and 4. The effect of the introduction of the lifetimes for momenta smaller than Q_c (i.e., $\sim 0.4a_0^{-1}$ in Na and $0.6a_0^{-1}$ in Al) mainly affects the intensity of the spectra, while the shape and the peak position remain practically unchanged. This can be explained by the fact that the main contributions to the spectra come from transitions close to the Fermi energy (where the quasiparticles have long lifetimes). For larger Q, the inclusion of lifetimes turns out to be crucial to obtain agreement with experiment. The improvement of TDLDA+LT over standard TDLDA is evident, and the spectra stand in good agreement with experiment. Beyond $2Q_c$, the inclusion of lifetimes still provides an improvement over standard TDLDA, but the agreement with experiment worsens. Here, the spectra appear overbroadened, which leads to an underestimate of the spectra at high energies, similar to what was found for silicon.[3,4]

Similar conclusions can be drawn for aluminum, the spectra of which are shown in Fig. 4. However, here the changes are less visible. For most momentum transfers we observe a slight improvement of the standard TDLDA results which are already in rather good agreement with the experimental results. However, for certain Q, e.g., $Q = 1.026a_0^{-1}$ in Fig. 4, the band-structure-related double-peak structure is becoming visible in standard TDLDA, while it is not yet present in the experimental spectrum. The effect of the lifetimes is here to wash out those structures, so as to bring the result into better agreement with experiment. For even larger Q, the band-structure effects creating the double peak are so strong that they cannot be washed out entirely by the lifetime effects, in agreement with the experimental findings.

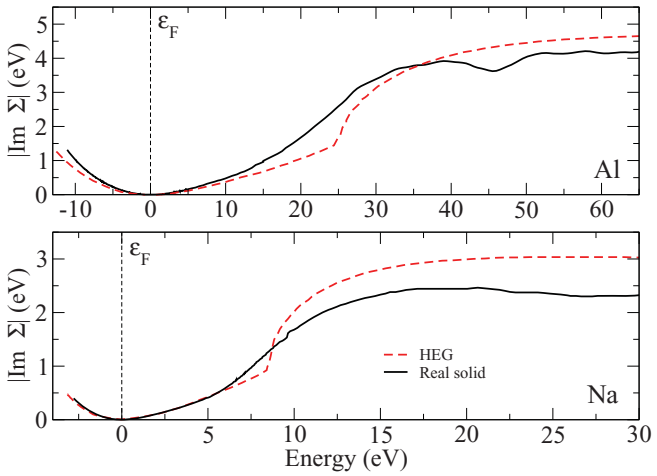

FIG. 5. (Color online) Imaginary part of the self-energy (damping, or inverse lifetime) for sodium and aluminum. The HEG curves are from Ref. 54, real-solid results for Na are those of Ref. 53, and the actual lifetimes for Al have been calculated by us with *GW* contour deformation and averaged over the BZ.

Besides broadening the spectra, the inclusion of lifetime effects has been shown to create a double-peak structure by itself in the case of the HEG. Figure 5 shows the lifetimes for the real solid compared with those of the HEG at the same density. The HEG dampings (imaginary parts of the self-energies), unlike those of the real solid, display a sudden increase at the energy at which the deexcitation by plasmon creation starts to be allowed.[55] This sudden change of slope has been addressed by Rahman and Vignale [24] as being responsible for the creation of the double peak in the $S(\mathbf{Q},\omega)$ of the HEG, therefore attributing it to correlation effects. In the real solid, interband transitions widen the plasmon peak and smooth the imaginary part of Σ.[53] As a consequence, our spectra calculated within TDLDA for Na including the lifetimes do not show the double peak predicted by Rahman and Vignale,[24] notwithstanding the fact that the RPA results for $S(\mathbf{Q},\omega)$ are very close to those of the HEG.

In fact, we observe the damping-induced double-peak structure in our HEG spectra for Q larger than $2Q_c$ (not shown), thus confirming Rahman and Vignale's result. Interestingly, the double peak is also present in the TDLDA calculation with lifetime inclusion in sodium when the lifetimes are approximated with those of the HEG. This is seen most clearly for the largest Q in Fig. 3. By contrast, when the actual lifetimes, calculated for the real solid and thus without the slope discontinuity, are used, the double-peak structure is not present and the spectra stand in good agreement with experiment.

We conclude that the double-peak structure in aluminum is clearly due to band-structure effects. It is washed out by the lifetime inclusion, but it survives at intermediate and large momentum transfers. In sodium, the very weak band-structure effect visible in RPA and TDLDA calculations is completely washed out by the lifetime effects. The latter themselves are not inducing a double peak in the solid, because the actual damping does not show the abrupt change of the slope typical of the HEG.

C. Calculations with different kernels

The inclusion of the lifetimes via the modified independent-particle polarizability χ_0^{LT} is approximate and not, strictly speaking, justified in the framework of linear-response TDDFT. There, the basic quantity is the Kohn-Sham independent-particle polarizability χ_0, which contains only real energies, while all exchange-correlation effects in the response should be introduced by the kernel. A brief discussion about this point applied to silicon can be found in Ref. 4, where it has been shown that a kernel introducing the lifetime effects is expected to present nonlocalities in time (explicit frequency dependence) and in space (wave-vector dependence), unlike the TDLDA kernel. The explicit frequency dependence is connected, via the Kramers-Kronig relations, with the presence of an imaginary part. In the following, we investigate the performance of existing kernels that show these properties, in order to determine their ability to describe lifetime effects improving the agreement with experiment.

A frequency-dependent kernel is the one proposed by Gross and Kohn,[10] which is a dynamical generalization of the TDLDA. It does have an imaginary part. We use this kernel in the same way as standard TDLDA, i.e., from the density we determine the kernel using the locality in real space, later transforming it into the reciprocal space. The results are shown in Figs. 6 and 7. The Gross-Kohn results are very close to standard TDLDA for both Na and Al; the differences are limited to a slight broadening of the spectra. The agreement with experiment remains poor.

To test the effect of a Q-dependent kernel we considered the Hubbard [11] and the Corradini *et al.*[12] kernels. In these cases we applied the kernels for the HEG with the corresponding density of Na or Al (i.e., the kernel is a diagonal matrix in **G**,**G**' and the diagonal elements depend only on $|\mathbf{q}+\mathbf{G}|$). The results of the calculation are plotted in Figs. 6 and 7. The Hubbard kernel moves the plasmon dispersion in the right direction compared to RPA when the momentum transfer is smaller than Q_c (i.e., $\sim 0.4a_0^{-1}$ in Na and $0.6a_0^{-1}$ in Al). In this range, it yields results similar to the TDLDA. On the other hand, as soon as Q increases beyond Q_c, the Hubbard kernel performs distinctly less well than the TDLDA, although an improvement with respect to the RPA remains. Similar conclusions hold for the Corradini *et al.* kernel which, however, stays close to the TDLDA result for large Q. None of the kernels obtain the quality of the TDLDA+LT results.

IV. THE PLASMON DISPERSION

In Fig. 8 we show the plasmon dispersion, i.e., the plasmon energy as a function of momentum transfer, calculated with the different approximations. The plasmon position has been determined as the energy corresponding to the maximum of $S(\mathbf{Q},\omega)$.

For both materials, but in particular for sodium, the available theoretical results within RPA and TDLDA from the literature [6] provide a poor description of the experimental results. This is particularly the case for larger momentum transfers. As in the case of the loss spectra, TDLDA with the additional inclusion of the lifetime effects is by far superior to all the other approximations considered in the present work.

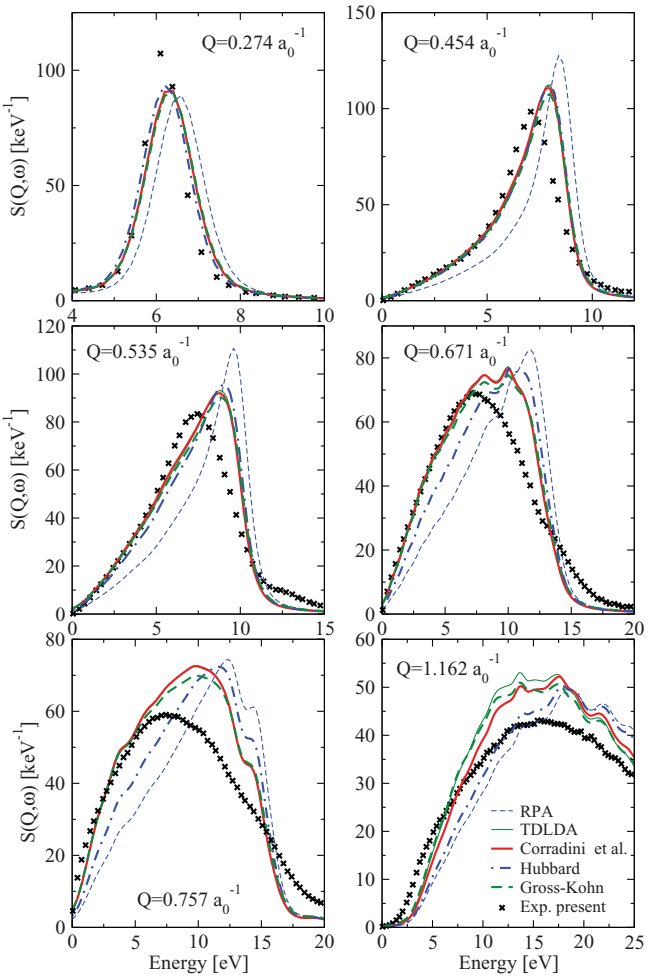

FIG. 6. (Color online) Comparison of experimental and calculated dynamical structure factor for sodium. Calculation are performed with the TDLDA, the Gross-Kohn, the Hubbard, and the Corradini *et al*. kernels ($Q_c \simeq 0.4a_0^{-1}$). Note that different energy scales are used in the different panels.

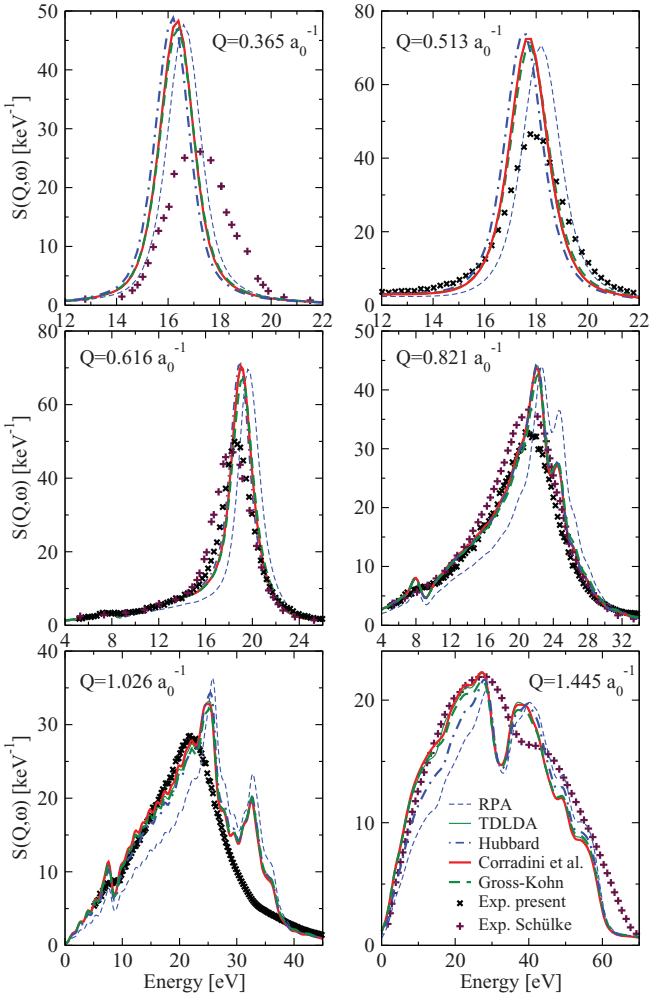

FIG. 7. (Color online) Same as Fig. 6 but for aluminum ($Q_c \simeq 0.6a_0^{-1}$).

The inclusion of the lifetimes leads to a great improvement in the agreement with experiment, especially for $Q > Q_c$. The effect is more visible in sodium than in aluminum.

As for the effect of the different kernels, TDLDA, the Gross-Kohn, and the Corradini *et al*. kernels improve upon the RPA result for all momentum transfers. The Hubbard kernel performs very well for $Q < Q_c$, while for $Q > Q_c$ it provides results poorer than the TDLDA. These findings are similar to what was already observed for the HEG.[56] The effect of the non-LDA kernels is more evident for sodium than for aluminum.

V. CONCLUSIONS

We have studied the dynamic response of sodium and aluminum within time-dependent density-functional theory using different approximations. In particular, we have calculated the dynamical structure factor and the plasmon dispersion. While for Al several experimental and theoretical results existed previously, no *ab initio* calculations of the dynamical structure factor of Na were available prior to our work. In both materials, RPA provides a very poor description of the spectra. TDLDA improves the agreement with experiment, although the spectra are still poor for sodium. The core polarization does not change the spectra appreciably. For aluminum, the TDLDA spectra stand in decent agreement with experiment, although within the TDLDA the well-known double-peak structure develops at slightly smaller Q than is seen in the experiment.

The approximate introduction of electron and hole lifetimes via the modified χ_0^{LT} greatly improves the spectra, bringing them into good agreement with experiment. Only for very large momentum transfers, deviations remain, similarly to what has been found earlier for silicon. The plasmon dispersion is likewise greatly improved and stands now in rather good agreement with the experimental results.

The double-peak structure developing at $Q \gtrsim 1.5Q_c$ in aluminum is clearly due to band-structure effects. It is partially washed out by the lifetime effects. The latter do not, by themselves, lead to a double-peak structure as they do in the case of the homogeneous electron gas, because no slope discontinuity is present in the lifetimes of the real materials. In fact, replacing the true Na lifetimes with those of the HEG does lead to a double-peak structure in the TDLDA+LT spectra.

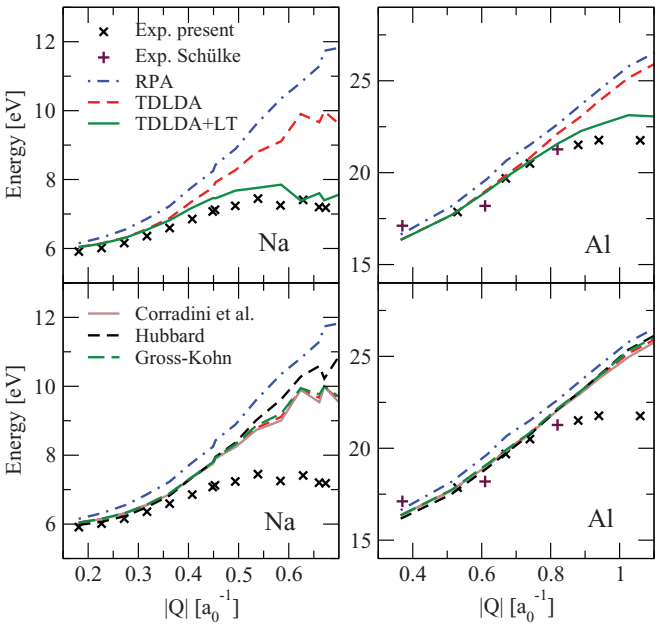

FIG. 8. (Color online) Plasmon dispersion of sodium (left-hand side) and aluminum (right-hand side). The plasmon cutoff vector Q_c is $\sim 0.4 a_0^{-1}$ in Na and $0.6 a_0^{-1}$ in Al.

The lifetime inclusion in χ_0^{LT} being approximate, we have studied the performance of existing nonlocal or time-dependent kernels. We find that the Gross-Kohn kernel, as well as the Hubbard and the Corradini *et al*. local-field factors, slightly improve upon the RPA results. However, none of them is able to achieve an agreement with experiment similar to that obtained by the inclusion of lifetimes in our TDLDA+LT calculations. This is clearly visible in both the spectra and the plasmon dispersion.

ACKNOWLEDGMENTS

We acknowledge useful discussions with R. Del Sole, N. Manini, A. Marini, V. Nazarov, F. Sottile, V. Olevano, and G. Vignale. The work was supported by the European Union through the ETSF e-I3 Grant No. INFRA-2007-211956. Beam time was provided by the European Synchrotron Radiation Facility. This work has been performed using HPC resources from GENCI-IDRIS (Grant No. 2009-544), as well as from CINECA through the *Calcolo per la Fisica della Materia* initiative. H.-Ch.W. acknowledges support from the European Union through the individual Marie Curie Intra-European Grant No. MEIF-CT-2005-025067, as well as from the Physics Department of the Ecole Polytechnique, Palaiseau, France. T.P. was supported by the Academy of Finland via Contract No. 1127462. S.H. was supported by Research Funds of the University of Helsinki, Contract No. 490076.

*marco.cazzaniga@unimi.it
†The CINaM is associated with the Universities of Aix-Marseille II and III.

[1] E. Runge and E. K. U. Gross, Phys. Rev. Lett. **52**, 997 (1984).
[2] S. Botti, A. Schindlmayr, R. Del Sole, and L. Reining, Rep. Prog. Phys. **70**, 357 (2007).
[3] H.-Ch. Weissker, J. Serrano, S. Huotari, F. Bruneval, F. Sottile, G. Monaco, M. Krisch, V. Olevano, and L. Reining, Phys. Rev. Lett. **97**, 237602 (2006).
[4] H.-Ch. Weissker, J. Serrano, S. Huotari, E. Luppi, M. Cazzaniga, F. Bruneval, F. Sottile, G. Monaco, V. Olevano, and L. Reining, Phys. Rev. B **81**, 085104 (2010).
[5] I. G. Gurtubay, J. M. Pitarke, W. Ku, A. G. Eguiluz, B. C. Larson, J. Tischler, P. Zschack, and K. D. Finkelstein, Phys. Rev. B **72**, 125117 (2005).
[6] A. A. Quong and A. G. Eguiluz, Phys. Rev. Lett. **70**, 3955 (1993).
[7] J. Z. Tischler, B. C. Larson, P. Zschack, A. Fleszar, and A. G. Eguiluz, Phys. Status Solidi B **237**, 280 (2003).
[8] G. Onida, L. Reining, and A. Rubio, Rev. Mod. Phys. **74**, 601 (2002), and references therein.
[9] B. C. Larson, J. Z. Tischler, W. Ku, C.-C. Lee, O. D. Restrepo, A. G. Eguiluz, P. Zschack, and K. D. Finkelstein, Phys. Rev. Lett. **99**, 026401 (2007).
[10] E. K. U. Gross and W. Kohn, Phys. Rev. Lett. **55**, 2850 (1985).
[11] G. D. Mahan, *Many Particle Physics* (Plenum, New York, 1981).
[12] M. Corradini, R. Del Sole, G. Onida, and M. Palummo, Phys. Rev. B **57**, 14569 (1998).
[13] W. Schülke, H. Schulte-Schrepping, and J. R. Schmitz, Phys. Rev. B **47**, 12426 (1993).
[14] B. C. Larson, J. Z. Tischler, E. D. Isaacs, P. Zschack, A. Fleszar, and A. G. Eguiluz, Phys. Rev. Lett. **77**, 1346 (1996).
[15] B. C. Larson, J. Z. Tischler, E. D. Isaacs, P. Zschack, A. Fleszar, and A. G. Eguiluz, J. Phys. Chem. Solids **61**, 391 (2000).
[16] A. vom Felde, J. Sprösser-Prou, and J. Fink, Phys. Rev. B **40**, 10181 (1989).
[17] J. P. Hill, C.-C. Kao, W. A. C. Caliebe, D. Gibbs, and J. B. Hastings, Phys. Rev. Lett. **77**, 3665 (1996).
[18] S. Huotari, C. Sternemann, W. Schülke, K. Sturm, H. Lustfeld, H. Sternemann, M. Volmer, A. Gusarov, H. Müller, and G. Monaco, Phys. Rev. B **77**, 195125 (2008).
[19] S. Huotari, M. Cazzaniga, H.-Ch Weissker, T. Pylkkanen, H. Muller, L. Reining, G. Onida, and G. Monaco, Phys. Rev. B **84**, 075108 (2011).
[20] A. Fleszar, A. A. Quong, and A. G. Eguiluz, Phys. Rev. Lett. **74**, 590 (1995).
[21] W. Schülke, H. Nagasawa, S. Mourikis, and P. Lanzki, Phys. Rev. B **33**, 6744 (1986).
[22] E.-N. Foo and J. J. Hopfield, Phys. Rev. **173**, 635 (1968).
[23] K. Sturm and L. E. Oliveira, Phys. Rev. B **30**, 4351 (1984).
[24] S. Rahman and G. Vignale, Phys. Rev. B **30**, 6951 (1984).
[25] G. Mukhopadhyay, R. K. Kalia, and K. S. Singwi, Phys. Rev. Lett. **34**, 950 (1975).
[26] K. Awa, H. Yasuhara, and T. Asahi, Solid State Commun. **38**, 1285 (1981).
[27] K. Awa, H. Yasuhara, and T. Asahi, Phys. Rev. B **25**, 3687 (1982).

[28]K. Awa, H. Yasuhara, and T. Asahi, Phys. Rev. B **25**, 3670 (1982).
[29]F. Yoshida, S. Takeno, and H. Yasuhara, Prog. Theor. Phys. **64**, 40 (1980).
[30]H. De Raedt and B. De Raedt, Phys. Rev. B **18**, 2039 (1978).
[31]F. Green, D. N. Lowy, and J. Szymański, Phys. Rev. Lett. **48**, 638 (1982).
[32]F. Green, D. Neilson, and J. Szymański, Phys. Rev. B **31**, 5837 (1985).
[33]J. Hong and M. H. Lee, Phys. Rev. Lett. **55**, 2375 (1985).
[34]G. Niklasson, A. Sjölander, and F. Yoshida, J. Phys. Soc. Jpn. **52**, 2140 (1983).
[35]W. Schülke, *Electron Dynamics by Inelastic X-Ray Scattering* (Oxford University Press, New York, 2007).
[36]L. Van Hove, Phys. Rev. **95**, 249 (1954).
[37]D. Pines and P. Nozieres, *The Theory of Quantum Liquids*, Vol. 1 (Benjamin, New York, 1966).
[38]S. L. Adler, Phys. Rev. **126**, 413 (1962).
[39]N. Wiser, Phys. Rev. **129**, 62 (1963).
[40]The ABINIT code is a common project of the Université Catholique de Louvain, Corning Incorporated, and other contributors [http://www.abinit.org].
[41]X. Gonze, G. M. Rignanese, M. Verstraete, J. Beuken, Y. Pouillon, R. Caracas, F. Jollet, M. Torrent, G. Zerah, M. Mikami *et al.*, Z. Kristallogr. **220**, 558 (2005).
[42]X. Gonze, B. Amadon, P. M. Anglade, J. M. Beuken, F. Bottin, P. Boulanger, F. Bruneval, D. Caliste, R. Caracas, M. Côté *et al.*, Comput. Phys. Commun. **180**, 2582 (2009).
[43]N. Troullier and J. L. Martins, Phys. Rev. B **43**, 1993 (1991).
[44]V. Olevano *et al.* [http://www.dp-code.org].
[45]R. Verbeni, T. Pylkkänen, S. Huotari, L. Simonelli, G. Vankó, K. Martel, C. Henriquet, and G. Monaco, J. Synchrotron Radiat. **16**, 469 (2009).
[46]K. Sturm, Adv. Phys. **31**, 1 (1982).
[47]K. Sturm and L. E. Oliveira, Phys. Rev. B **24**, 3054 (1981).
[48]C. Sternemann, S. Huotari, G. Vankó, M. Volmer, G. Monaco, A. Gusarov, H. Lustfeld, K. Sturm, and W. Schülke, Phys. Rev. Lett. **95**, 157401 (2005).
[49]K. Sturm and A. Gusarov, Phys. Rev. B **62**, 16474 (2000).
[50]P. Romaniello, D. Sangalli, J. A. Berger, F. Sottile, L. G. Molinari, L. Reining, and G. Onida, J. Chem. Phys. **130**, 044108 (2009).
[51]H.-Ch. Weissker, M. Cazzaniga, L. Caramella, E. Luppi, X. Lopez-Lozano, G. Onida, and L. Reining (unpublished).
[52]S. Lebègue, B. Arnaud, M. Alouani, and P. E. Bloechl, Phys. Rev. B **67**, 155208 (2003).
[53]J. S. Dolado, V. M. Silkin, M. A. Cazalilla, A. Rubio, and P. M. Echenique, Phys. Rev. B **64**, 195128 (2001).
[54]Kenneth W.-K. Shung, B. E. Sernelius, and G. D. Mahan, Phys. Rev. B **36**, 4499 (1987).
[55]J. J. Quinn, Phys. Rev. **126**, 1453 (1962).
[56]K. Tatarczyk, A. Schindlmayr, and M. Scheffler, Phys. Rev. B **63**, 235106 (2001).